Hot-Electron–Phonon Interaction in the Nonparabolic Conduction Band of Degenerate InSb at 4.2 K*

H. Kahlert and G. Bauer
Ludwig Boltzmann-Institut für Festkörperphysik and Institut für Angewandte Physik der Universität Wien, A-1090 Vienna, Austria
(Received 10 July 1972)

Adopting the Kane model of the nonparabolic conduction band of InSb, calculations of the energy-loss rates of the electrons to acoustic modes via deformation potential and piezoelectric coupling and to polar optical modes are performed. Use is made of matrix elements which take into account p-function admixture and static screening of the electron-phonon interaction. The applicability of this theoretical approach to experiments at 4.2 K in strongly degenerate n-InSb is examined. Measurements of the electric-field-dependent amplitudes of the Shubnikov–de Haas effect with $B \| j$ are used to determine the dependence of the electron temperature on the electric field up to 1.7 V/cm. Theoretical values of the energy-loss rates are found on averaging over the Fermi distribution at an elevated electron temperature T_e. A combination of deformation-potential scattering and piezoelectric scattering accounts for the energy-loss rate below $T_e = 12$ K. A value of the deformation-potential constant of 6.9 ± 0.4 eV is used to fit the calculated energy-loss rates to the experimental data. Above $T_e = 24$ K, polar-optical-phonon scattering is the dominant mechanism. Between 12 and 24 K, there remains a difference between experiment and theory which is attributed to a two-phonon-scattering process.

I. INTRODUCTION

The mechanism of electron energy transfer to the crystal lattice[1] in n-type InSb at low temperature was studied originally by Sladek.[2] He considered the interaction of the electrons with the piezoelectric potential of the acoustic phonons and with polar optical phonons. Since this early attempt, much work as been concerned with this problem. Lifshits *et al.*[3] have pointed out the necessity to take acoustic deformation-potential scattering into consideration. Kinch[4,5] has demonstrated the importance of screening effects for the electron–acoustic-phonon interaction. Measurements of the dependence of the mobility on the electric field by Sandercock[6] and by Whalen and Westgate[7] were undertaken to get insight into these mechanisms. Maneval *et al.*[8] obtained the average electron-energy-loss rate as a function of the electric field using a sophisticated experimental technique, and were the first to point out the difficulty of comparing these data with the usual theoretical approach involving perturbation theory and the Boltzmann transport equation. This point was later stressed also by Tsidilkovskii and Demchuk.[9] Szymanska and Maneval[10] and Martin and Mead[11] have ignored these difficulties and have deduced values for the conduction-band deformation-potential constant by comparing the experimentally obtained energy-loss rate of the electron gas to the lattice with theoretical expressions given by Kogan.[12] Stradling *et al.*[13] and Martin and Mead[11] have focused attention on the fact that a combination of deformation-potential, piezoelectric, and polar-optical-phonon scattering is not sufficient to explain the experimentally observed temperature dependence of the energy-loss rate, and another energy-loss mechanism has to be taken into account. Two-phonon mechanisms have been proposed to explain the remaining discrepancy.[11,13]

If one intends to compare any semiconductor transport experiment with the usual theoretical formulation of the electron-phonon interaction based upon the adiabatic principle[14] and perturbation theory, one has to prove carefully whether these approximations are justified or not. The adiabatic principle fails to be acceptable under conditions where the period of a lattice wave is shorter than the time τ between successive collisions of an electron, which means that the condition

$$\hbar/k_B T < \tau \tag{1}$$

is not satisfied. Peierls[15] has pointed out that the Boltzmann equation and the use of perturbation theory are not justified unless this inequality is satisfied. According to an argument given by Landau and Peierls,[16] $k_B T$ can be replaced by the Fermi energy ϵ_F measured from the nearest band edge in metals or degenerate semiconductors so that the theory should not break down as long as

$$\hbar/\epsilon_F < \tau \ . \tag{2}$$

Directly related to this condition is

$$1 < k l_e \ , \tag{3}$$

which states that the mean free path of an electron between successive collisions should be greater

than its wavelength: The wave function of an electron should last at least a whole oscillation before it can be assigned a whole wavelength. In degenerate semiconductors, k is replaced by k_F, the electron wave vector at the Fermi surface.

Several attempts have been made to bypass these theoretical difficulties under conditions where Eq. (1) is not satisfied. Relaxation effects in the electron-phonon interaction have been explicitly introduced either phenomenologically by adding a relaxation term to the density-matrix equation or by the replacement of the usual Fermi "Golden Rule" by a Wigner–Breit-type theory.[17] However, an exact quantum treatment of this case remains an unsolved problem.

The outlined difficulties of a comparison between experiment and theory are overcome by investigating sufficiently degenerate high-mobility semiconductors. If the value of ϵ_F is high enough, conditions (2) and (3) can easily be satisfied.

Furthermore, any transport theory dealing with the conduction band of InSb has to consider the nonparabolic shape of the $\epsilon(\vec{k})$ relation as derived by Kane.[18] Kane's theory results from taking into account the interaction of the valence bands and the conduction band through the $\vec{k}\cdot\vec{p}$ terms of the Hamiltonian. The $\vec{k}$-independent spin-orbit interaction was also considered exactly. Using this theory, Ehrenreich[19,20] performed calculations of the mobility in the conduction band of InSb by combining polar-optical-phonon, electron-hole, and acoustic-phonon scattering in the temperature range above 200 K. He also considered for the first time the influence of static screening on the electron–polar-optical-phonon interaction and the admixture of p-like components into the total wave function of the electrons in the conduction band. In a recent report, Zawadzki and Szymanska[21] have presented a detailed analysis of elastic electron scattering in InSb-type semiconductors and have given expressions for the matrix elements which include the effect of static screening and of the p-function admixture for scattering by ionized impurities, polar optical phonons, and acoustic phonons for both types of coupling. For the nondegenerate case, the rate of change of momentum and energy of the electrons by polar-optical-phonon, acoustic-phonon, and ionized-impurity scattering was calculated by Stokoe and Cornwell,[22] including the effect of mixing of Bloch states.

It is the purpose of the present paper to derive exact expressions for the energy-loss rates in the nonparabolic conduction band of InSb for scattering by polar optical modes and acoustic modes via the deformation potential and the piezoelectric interaction. Static screening and admixture of p-like components will be included in the calculations. We compare these theoretical results with measurements of the dependence of the energy-loss rates on the electron temperature. The decrease of the amplitudes of the longitudinal Shubnikov–de Haas (SdH) effect is used as a measure of the increase in the electron temperature with applied electric field.[23–25] We use degenerate n-InSb samples with $\eta = \epsilon_F/k_B T_e = 100 \pm 3$ at 4.2 K and high mobility so that Eqs. (2) and (3) are satisfied and a comparison of the experiment with the usual transport theory is justified. From this comparison we deduce a value for the deformation-potential constant of the conduction band of n-InSb.

In Sec. II, we start with the transition probabilities given by Zawadzki and Szymanska[21] and arrive at expressions for the energy-loss rates for polar-optical-phonon, deformation-potential, and piezoelectric scattering. These expressions are averaged numerically over the Fermi–Dirac distribution. In Sec. III, the experimental techniques are described. In Sec. IV, the experimental results are presented and their interpretation in terms of an electron-temperature model is given. In Sec. V, we compare the experimental results with numerical calculations of the theoretical energy-loss rates. From this comparison we deduce a value for the conduction-band deformation-potential constant and discuss this value reviewing the results of other experimental determinations of this parameter.

II. THEORY

A. Carrier Concentration, Screening Length, and Ionized-Impurity Scattering in a Nonparabolic Band

Using the simplified Kane formula[18]

$$\epsilon(\vec{k}) = -A^{1/2} + (A + Bk^2)^{1/2} , \tag{4}$$

with $A = \frac{1}{4}\epsilon_g^2$ and $B = \epsilon_g \hbar^2/2m_c$, where m_c is the effective mass at the bottom of the conduction band and ϵ_g the energy gap, the electron concentration becomes[26,27]

$$n = \frac{1}{3\pi^2}\left(\frac{2m_c k_B T}{\hbar^2}\right)^{3/2} \int_0^\infty -\frac{\partial f_0}{\partial x}\left(x + \frac{k_B T}{\epsilon_g}x^2\right)^{3/2} dx , \tag{5}$$

with $x = \epsilon/k_B T$, ϵ being the electron energy, and $f_0 = 1/(e^{x-\eta}+1)$. In Fig. 1 the Fermi energy ϵ_F is plotted as a function of temperature with the carrier concentration n as a parameter. The constants[28–32] used in the numerical calculations are listed in Table I.

The screening length λ which appears in the long-range interactions is given by[26]

$$\frac{1}{\lambda^2} = \frac{2e^2}{\pi\kappa_0 k_B T}\left(\frac{2m_c k_B T}{\hbar^2}\right)^{3/2} \times \int_0^\infty -\frac{\partial f_0}{\partial x}\left(x + \frac{k_B T}{\epsilon_g}x^2\right)^{1/2}\left(1 + \frac{2k_B T}{\epsilon_g}x\right) dx, \tag{6}$$

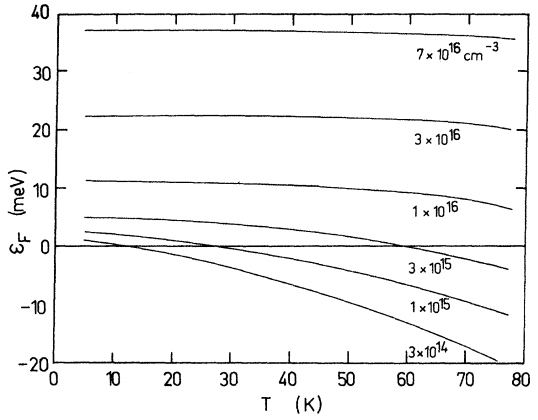

FIG. 1. Fermi energy of n-InSb as a function of temperature for various carrier concentrations between 3×10^{14} and 7×10^{16} cm^{-3}.

κ_0 being the static dielectric constant. The dependence of $1/\lambda^2$ on temperature with the carrier concentration as a parameter is shown in Fig. 2.

The relaxation time for ionized-impurity scattering for an electron with wave vector $\vec{k}$ has the form[21]

$$\tau_i = \frac{\kappa_0^2 \hbar}{2\pi e^4 N_I F_i}\left(\frac{d\epsilon}{dk}\right) k^2 \,. \tag{7}$$

Using the relation valid for a spherical band,

$$\frac{1}{m} = \frac{1}{\hbar^2 k}\left(\frac{d\epsilon}{dk}\right) , \tag{8}$$

the mobility $\langle \mu_i \rangle = e\langle \tau_i/m \rangle$ is obtained by averaging over the distribution function in the form

$$\langle \mu_i \rangle = \frac{\kappa_0^2 B^2}{6\pi^3 e^3 \hbar m N_I k_B T} \times \int_0^\infty \frac{k^7}{(k^2 + A/B)\,(A + Bk^2)^{1/2} F_i} f_0(k)[1 - f_0(k)]\, dk \,, \tag{9}$$

where, according to Ref. 21, F_i is given by

$$F_i(\xi, L) = \ln(\xi + 1) - \frac{\xi}{\xi + 1}$$

TABLE I. Constants used in the numerical calculation.

$m_c = 0.0139 m_0$	Effective mass[a]
$d = 5.82$ g/cm^3	Mass density
$e_{14}^2 = 5.62\times10^8$ dyn/cm^2	Piezoelectric modulus[b]
$\Theta_D = 278$ K	Debye temperature[c]
$\kappa_0 = 17.88$	Static dielectric constant[c]
$\kappa_\infty = 15.68$	Optical dielectric constant[c]
$\epsilon_g = 0.235$ eV	Energy gap[d]
$\Delta = 0.82$ eV	Spin-orbit splitting[e]

[a]Reference 28.
[b]Reference 29.
[c]Reference 30.
[d]Reference 31.
[e]Reference 32.

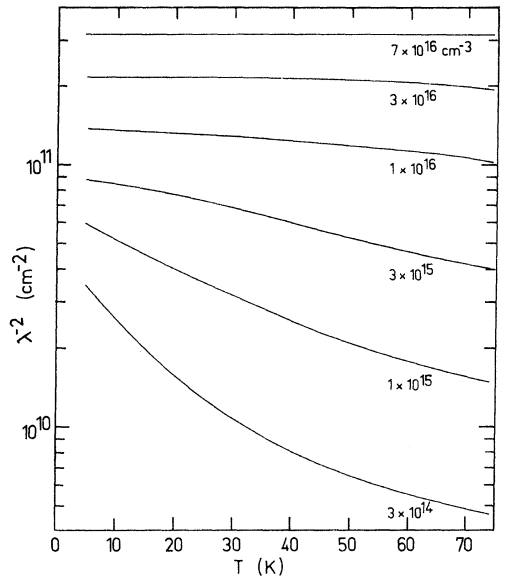

FIG. 2. Inverse square of the screening length as a function of temperature for various carrier concentrations between 3×10^{14} and 7×10^{16} cm^{-3}.

$$- (4L - gL^2)\left(1 + \frac{1}{\xi+1} - \frac{2}{\xi}\ln(\xi+1)\right) + \tfrac{1}{2}L^2(4-g)\left(1 - \frac{4}{\xi} + \frac{6}{\xi^2}\ln(\xi+1) - \frac{2}{\xi(\xi+1)}\right) , \tag{10}$$

with the abbreviations

$$L = \frac{\epsilon}{\epsilon_g + 2\epsilon} \,, \quad \beta^2 = \frac{\Delta^2}{(\Delta + \epsilon_g)(\Delta + \frac{3}{2}\epsilon_g)} \,, \quad \gamma^2 = \frac{\Delta + \frac{3}{2}\epsilon_g}{\Delta + \epsilon_g} \,,$$

$$\xi = (2k\lambda)^2 \,, \qquad g = \tfrac{1}{9}\beta^2(16\gamma^2 - 8\beta\gamma + \beta^2) \,.$$

A numerical calculation of the ionized-impurity mobility and its dependence on temperature using Eq. (9) and the constants listed in Table I is shown in Fig. 3. The impurity density N_I and the screening density were assumed to be equal to the free-carrier density n. The parameter for the different curves is the electron concentration n. Although the impurity concentration is varied by more than two orders of magnitude, the theoretical mobility varies only by a factor of 30 at 75 K and only by a factor of 5 at 4.2 K. From this fact we understand why an increase of the electron concentration and hence of the Fermi energy is not necessarily connected with a drastic reduction of the relaxation time and enables one to satisfy condition (2).

B. Energy-Loss Rates in a Nonparabolic Band

1. General Procedure

The rate of change of carrier energy because of phonon scattering is obtained by subtracting the

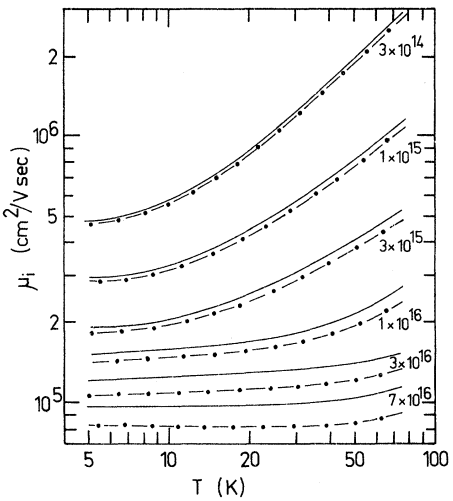

FIG. 3. Ionized-impurity mobility vs temperature. Impurity density N_I is assumed to be equal to the free-carrier density n for all concentrations: Solid lines, with p-function admixture; dash-dotted lines, without p-function admixture.

energy gain by absorption of phonons from the energy loss by emission of phonons.[1] For a phonon with wave vector $\vec{q}$, the gain is given by $\hbar uq$ times the probability $W_{\vec{k},\vec{k}+\vec{q}}$ of a phonon being absorbed; the loss is given by $\hbar uq$ times the probability $W_{\vec{k},\vec{k}-\vec{q}}$ of a phonon being emitted, where $\hbar uq$ is the phonon energy and u the sound velocity. These expressions have to be summed over all possible $\vec{q}$ yielding

$$\frac{d\epsilon}{dt}=\frac{V}{8\pi^3}\left(\int_{q_1^+}^{q_2^+}\hbar uq\,W_{\vec{k},\vec{k}+\vec{q}}\,d^3q-\int_{q_1^-}^{q_2^-}\hbar uq\,W_{\vec{k},\vec{k}-\vec{q}}\,d^3q\right). \tag{11}$$

In order to obtain the average energy-loss rate this expression has to be averaged over the distribution function $f(\vec{k})$ in the form

$$\left\langle\frac{d\epsilon}{dt}\right\rangle=\frac{2}{8\pi^3 n}\int_{-\infty}^{\infty}f(\vec{k})\frac{d\epsilon}{dt}\,d^3k\,. \tag{12}$$

This can only be done numerically since $f(\vec{k})$ is the Fermi–Dirac distribution function and $d\epsilon/dt$ is a complicated function of $\vec{k}$. The use of this distribution at an elevated electron temperature T_e is well justified in our case because of the strong degeneracy of the n-InSb samples we have studied experimentally.

The energy-loss rates in a parabolic band were given by Conwell[1] for various scattering mechanisms. In the case of a nonparabolic band one has to consider the effect of the band shape not only in the density of states but also in the scattering probability. Therefore one has to take into account the proper electron wave functions resulting from the nonparabolicity of the $\epsilon(\vec{k})$ relation. This was first pointed out by Ehrenreich[20] who used the complete wave functions when solving the Boltzmann equation by a variational procedure. Later Matz[33] considered the admixture of p-like components to the wave function in calculating the current-density-field-strength characteristic for n-InSb.

In the present paper we follow the procedure outlined by Zawadzki and Szymanska[21] who calculated the mobility in nonparabolic semiconductors for various scattering mechanisms. We use the transition probabilities calculated by these authors but take into account the inelasticity of the electron-phonon collisions since we calculate energy-loss rates.

2. *Polar-Optical-Phonon Scattering*

The transition probability for the absorption (upper sign) and emission (lower sign) of an optical phonon is given by

$$W^{\mathrm{po}}_{\vec{k},\vec{k}\pm\vec{q}}=w^{\mathrm{po}}_{\pm}(k,q)\,(N_q+\tfrac{1}{2}\mp\tfrac{1}{2})\,\delta(\epsilon(|\vec{k}\pm\vec{q}|)-\epsilon(|\vec{k}|)\mp\hbar\omega)\times[1-f(\epsilon\pm\hbar\omega)]\,, \tag{13}$$

where, according to Ref. 21,

$$w^{\mathrm{po}}_{\pm}(k,q)=\frac{4\pi^2e^2\omega}{V}\left(\frac{1}{\kappa_\infty}-\frac{1}{\kappa_0}\right)\left(\frac{\lambda^2q}{1+\lambda^2q^2}\right)^2\times(|I^{\pm}_{1/2,1/2}|^2+|I^{\pm}_{1/2,-1/2}|^2)\,. \tag{14}$$

N_q is the phonon occupation number, ω the frequency of the longitudinal phonons, and κ_∞ the optical dielectric constant. The terms $I_{jj'}$ are given by[21]

$$I^{\pm}_{1/2,1/2}(q)=1-2(b^2+c^2)\,(\cos^2\theta)_{\pm} \tag{15}$$

and

$$I^{\pm}_{1/2,-1/2}(q)=\pm\,2b(\tfrac{1}{2}b-c\sqrt{2})\,(\cos\theta)_{\pm}(\sin\theta)_{\pm}\,e^{i\phi}\,, \tag{16}$$

with the abbreviations

$$a^2=\frac{\epsilon_g+\epsilon}{\epsilon_g+2\epsilon-\alpha\epsilon}\,,\quad b^2=\frac{1}{3}\,\frac{\epsilon}{\epsilon_g+2\epsilon-\alpha\epsilon}\,\beta^2\,,$$
$$c^2=\frac{2}{3}\,\frac{\epsilon}{\epsilon_g+2\epsilon-\alpha\epsilon}\,\gamma^2\,,\quad \alpha=\frac{\Delta\epsilon_g}{2(\Delta+\frac{3}{2}\epsilon_g)(\Delta+\epsilon_g)}\,, \tag{17}$$

where Δ is the spin-orbit splitting. We follow the common procedure of performing the q integration in spherical coordinates with $d^3q=q^2\,dq\sin\theta\,d\theta\,d\phi$. Since the initial $\vec{k}$ vector can be taken along the z direction, the δ functions also contain θ as a variable. For the absorption and emission process, we obtain

$$(\cos\theta)_{\pm}=\frac{\pm\,C^2\mp Bq^2+2C(A+Bk^2)^{1/2}}{2Bkq}\,, \tag{18}$$

with $C=\hbar\omega$. After performing the θ integration the remaining integral is given by

$$\int_{q_1^{\pm}}^{q_2^{\pm}} w_{\pm}^{po}(k,q)\left[\frac{1}{q^2}\left(\frac{\pm C^3 \pm 2AC + 3C^2(A+Bk^2)^{1/2}}{2B^2k^2} \pm \frac{C}{B}\right) \mp \frac{C \pm (A+Bk^2)^{1/2}}{2Bk^2}\right] q^2\, dq\, 2\pi\,, \quad (19)$$

which is obtained by using

$$\int du\, \delta(f(u)) = \int \frac{du\, \delta(u-u_0)}{|\,\partial f/\partial u|_{u=u_0}}\,. \quad (20)$$

The limits of the q integration are

$$q_1^{\pm} < q < q_2^{\pm}\,,$$

with

$$q_1^{\pm} = \mp k \pm \{k^2 \pm [2C(A+Bk^2)^{1/2} \pm C^2]/B\}^{1/2}\,, \quad (21)$$
$$q_2^{\pm} = k + \{k^2 \pm [2C(A+Bk^2)^{1/2} \pm C^2]/B\}^{1/2}\,.$$

Finally, the optical-phonon absorption and emission probability for an electron with wave vector $\vec{k}$ is given by

$$\frac{V}{8\pi^3}\int_{q^{\mp}}^{q_2^{\pm}} W^{po}_{\vec{k},\vec{k}\pm\vec{q}}\, d^3q = (N_q + \tfrac{1}{2} \mp \tfrac{1}{2})e^2\omega\left(\frac{1}{\kappa_\infty} - \frac{1}{\kappa_0}\right) \times \int_{q_1^{\pm}}^{q_2^{\pm}} G_{\pm}(k,q)\, dq\,, \quad (22)$$

with

$$G_{\pm}(k,q) = \left(\frac{\lambda^2 q}{1+\lambda^2 q^2}\right)^2 \left(\frac{\pm C^3 \pm 2AC + 3C^2(A+Bk^2)^{1/2}}{2B^2k^2} \pm \frac{C}{B} \mp \frac{q^2[C \pm (A+Bk^2)^{1/2}]}{2Bk^2}\right)[1 - f(\epsilon \pm \hbar\omega)] \times (|I^{\pm}_{1/2,1/2}|^2 + |I_{1/2,-1/2}|^2)\,. \quad (23)$$

Neglecting the dispersion of the optical phonons, $\hbar u q = \hbar\omega$ has been taken outside the integral in Eq. (11).

3. Deformation-Potential Scattering

The transition probability for the absorption (upper sign) and the emission (lower sign) of an acoustic phonon of the νth branch is given by

$$W^{\nu}_{\vec{k},\vec{k}\pm\vec{q}} = w^{\nu}_{\pm}(k,q)(N_q + \tfrac{1}{2} \mp \tfrac{1}{2})\delta(\epsilon(|\vec{k}\pm\vec{q}|) - \epsilon(|\vec{k}|) \mp \hbar\omega^{\nu}_{\vec{q}}) \times [1 - f(\epsilon \pm \hbar\omega^{\nu}_{\vec{q}})]\,, \quad (24)$$

where[21]

$$w^{\nu}_{\pm}(k,q) = \frac{2\pi}{\hbar}\left(\frac{\hbar}{2Vd\omega^{\nu}_q}\right)\sum_{j'} |I^{\nu}_{jj'}(q)|^2\,. \quad (25)$$

The superscript $\nu = 1, 2, 3$ denotes one of the three possible polarizations (one longitudinal and two transverse branches). The $I_{jj'}$ were given in Ref. 21. The value used for $\cos\theta$ is that which makes the argument of the δ function vanish and is

$$(\cos\theta)_{\pm} = \frac{\pm\hbar^2 u_\nu^2 q \mp Bq + 2\hbar u_\nu (A+Bk^2)^{1/2}}{2Bk}\,. \quad (26)$$

The limits of the q integration are given by

$$0 < q < \frac{2k \pm [2\hbar u_\nu (A+Bk^2)^{1/2}]/B}{1 - \hbar^2 u_\nu^2/B} = q_2^{\pm}\,. \quad (27)$$

For example, the contribution of longitudinal phonons to the energy-loss rate has the form

$$\frac{V}{8\pi^3}\int_0^{q_2^{\pm}} \hbar u_1 q\left(\frac{\pm\hbar^3 u_1^3 q^3 \pm 2A\hbar u_1 q + 3\hbar^2 u_1^2 q^2 (A+Bk^2)^{1/2}}{2B^2k^2} \pm \frac{\hbar u_1 q}{B} \mp \frac{q^2[\hbar u_1 q \pm (A+Bk^2)^{1/2}]}{2Bk^2}\right) \times (N_q + \tfrac{1}{2} \mp \tfrac{1}{2})[1 - f(\epsilon \pm \hbar u_1 q)] w^1_{\pm}(q,k)\, dq\, 2\pi\,. \quad (28)$$

One has to consider the absorption and emission processes for one longitudinal ($\nu = 1$) and two transverse branches ($\nu = 2, 3$) and to combine them in the form

$$\frac{d\epsilon}{dt} = \frac{V}{8\pi^3}\sum_{\nu}\left(\int_0^{q_2^{\vec{}}} \hbar u_\nu q W_{\vec{k},\vec{k}+\vec{q}}\, d^3q - \int_0^{q_2^{\vec{}}} \hbar u_\nu q W_{\vec{k},\vec{k}-\vec{q}}\, d^3q\right). \quad (29)$$

The numerical calculations showed that the contribution of the transverse modes to the total energy-loss rate are negligibly small for the given experimental situation. We need therefore only the expressions for the $I^1_{jj'}$ for the longitudinal mode which according to Ref. 21 are given by

$$|I^1_{1/2,1/2}(q)|^2 = E_c^2 q^2\left\{a^2 + \frac{E_1 b^2}{E_c 2} + \frac{E_2}{E_c}\left(c^2 + \frac{b^2}{2}\right) - \frac{q^2}{4k^2}\left[\frac{E_1}{E_c}\left(c^2 + \frac{b^2}{2}\right) + \frac{E_2}{E_c}\left(5c^2 + \frac{b^2}{2}\right)\right] + \frac{q^4 E_2}{4k^4 E_c}\left(c^2 - \frac{b^2}{2}\right)\right\}^2 \quad (30)$$

and

$$|I^1_{1/2,-1/2}(q)|^2 = E_1^2 \frac{q^4}{4k^2}\left(1 - \frac{q^2}{4k^2}\right)b^2c^2\,. \quad (31)$$

The constant E_c plays the role of the deformation-potential constant. Following the arguments given by the above authors, $E_1 = \frac{29}{40}E_c$ and $E_2 = \frac{3}{40}E_c$ were taken.

4. Piezoelectric Scattering

The matrix element between the initial and final states for scattering by the piezoelectric potential of acoustic phonons is[21]

$$\langle \vec{k}', j', N'_{\vec{q}}|\, U\, |\vec{k}, j, N_{\vec{q}}\rangle = -\frac{8\pi e e_{14}}{\kappa_0}\left(\frac{\hbar}{2Vd\omega^{\nu}_q}\right)^{1/2} \times [\delta_{\vec{k}',\vec{k}+\vec{q}} N^{1/2}_{\vec{q}} - \delta_{\vec{k}',\vec{k}-\vec{q}}(N_{\vec{q}}+1)^{1/2}] \times K_\nu\left(\frac{\lambda^2 q^2}{1+\lambda^2 q^2}\right) I_{jj'}(q)\,, \quad (32)$$

where K_ν is given by

$$K_\nu = e^\nu_{ac\,1}\, e_2 e_3 + e^\nu_{ac\,2}\, e_3 e_1 + e^\nu_{ac\,3}\, e_1 e_2 \ , \tag{33}$$

with $\vec{e}^{\,\nu}_{ac}$ being the unit polarization vector of the acoustic wave and $\vec{e}$ the unit vector along its polarization direction. e_{14} denotes the piezoelectric modulus and the $I_{j,j'}$ are identical with the expressions given in Eqs. (15) and (16) for polar-optical-phonon scattering. The expressions for $(\cos\theta)_\pm$ are the same as for deformation-potential scattering as well as the limits for the q integration. As usual in calculations of the relaxation time, we take K_ν^2 outside the integral over $\vec{q}$. The averaging procedure is, as demonstrated by Kogan,[12]

$$\zeta = \textstyle\sum_\nu \int_\Omega K_\nu^2 d\Omega/2\pi \ . \tag{34}$$

For a cubic crystal, ζ is a number approximately equal to 0.4. The probabilities $W^{pi}_{\vec{k},\vec{k}\pm\vec{q}}$ are given by Eq. (24) but with

$$w^{pi}_\pm(k,q) = \frac{32\pi^2 e^2 e_{14}^2 \zeta}{\kappa_0^2}\ \frac{\hbar}{Vduq}\left(\frac{q^2\lambda^2}{1+q^2\lambda^2}\right)^2 \times\left(\left|I^\pm_{1/2,1/2}\right|^2 + \left|I^\pm_{1/2,-1/2}\right|^2\right) \ . \tag{35}$$

C. Oscillatory Magnetoresistance

The SdH effect can be observed under the following conditions:

$$\omega_c \tau \gg 1, \ \hbar\omega_c > k_B T_e \epsilon_F > \hbar\omega_c \ , \tag{36}$$

where $\omega_c = eH/m^*$, m^* is the cyclotron effective mass, and H represents the magnetic field. For this case several Landau levels whose spacing is $\hbar\omega_c$ are occupied, and changes in the applied magnetic field result in a passage of the Landau levels past the Fermi energy ϵ_F. Consequently an oscillatory behavior of the magnetoresistance is observed which is periodic in $1/H$. The theory of the longitudinal and transverse oscillatory magnetoresistance have been reviewed in Ref. 34. The theoretical expressions are

$$\frac{\Delta\rho}{\rho_0} = t\sum_{s=1}^{\infty}\left[b_s\left(\cos\frac{2\pi s\epsilon_F}{\hbar\omega_c} - \frac{\pi}{4}\right) + R\right] \ , \tag{37}$$

with

$$b_s = \frac{(-1)^s}{s^{1/2}}\left(\frac{\hbar\omega_c}{2\epsilon_F}\right)^{1/2} \frac{2\pi^2 s k_B T/\hbar\omega_c}{\sinh(2\pi^2 s k_B T/\hbar\omega_c)} \times \cos\pi\Xi s\, e^{-2\pi^2 k_B T_D/\hbar\omega_c} \ , \tag{38}$$

where ρ_0 is the zero-field resistivity, s the sth harmonic, and Ξ the ratio of the spin splitting to the Landau-level spacing. T_D denotes the nonthermal broadening temperature (Dingle temperature[34]). The term R is an additional series of oscillatory terms in the transverse magnetoresistance and is generally smaller than b_s. t is equal to 2.5 or 1 for the transverse or longitudinal case, respectively.

If the electron-temperature model is used to describe the influence of an electric field on the electron gas, the amplitudes M of the oscillations at different electric fields are related to each other by

$$\frac{M(E_1)}{M(E_2)} = \frac{M(T_{e,1})}{M(T_{e,2})} = \frac{\chi_1/\sinh\chi_1}{\chi_2/\sinh\chi_2} \ , \tag{39}$$

where $\chi_i = 2\pi^2 k_B T_{e,i}/\hbar\omega_c$. This equation is valid under the assumption that the Dingle temperature does not vary with the electric field and that the series in Eq. (37) can be approximated by its first term.

III. EXPERIMENTAL

Samples were prepared from n-type bulk single-crystal InSb having an electron concentration of 6.9×10^{16} cm^{-3} and a mobility of 74.500 cm^2/V sec at 4.2 K. In order to avoid contact effects, bridge-shaped samples have been prepared by the sand-blasting technique from lapped thin wafers and were subsequently etched. Typical sample dimensions are indicated in Fig. 4. Two current contacts, two potential contacts, and two Hall contacts were soldered to the samples with tin. The samples were placed within a variable temperature cryostat (2.4–77 K).

Ohmic measurements were made by using a Keithley 148 nanovoltmeter. Pulsed-current techniques were used to avoid sample heating for the non-Ohmic measurements. Voltage pulses of 500-nsec duration, a repetition rate of 10–50 Hz, and a rise time below 15 nsec were produced by a HP 214 pulse generator. In order to observe any variation of the conductivity with electric field, with magnetic field, and with time after application of the voltage pulse two Tektronix sampling oscilloscopes (561B, 3S1, 3T2 and 561A, 3S76, 3T77) were used. Two Keithley model 109 preamplifiers (rise time about 3 nsec) amplified the signals from the samples prior to feeding them into the oscilloscopes. The output signals of the oscilloscopes were fed into an HP 7004B x-y recorder. Using this recorder and the field sweep of the magnet coil, direct plots of the magnetoresistance versus H were obtained. The experiments were made under constant-current conditions.

IV. RESULTS AND ANALYSIS

A. Ohmic and Non-Ohmic Mobility

The Ohmic conductivity and the Hall effect were measured between 4.2 and 30 K. From these data a mobility increase with temperature was found which was less than 0.5%. To determine whether the electric fields employed in our SdH measurements produce any appreciable carrier concentration or mobility changes, electric fields up to

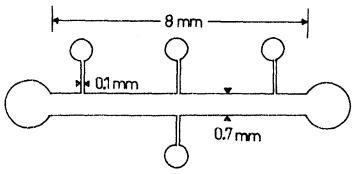

FIG. 4. Geometry of samples.

2 V/cm were applied as dc pulses to the samples. No conductivity change was observed within the experimental error (< 1%).

The Ohmic Hall data yielded a carrier concentration of 6.9×10^{16} cm^{-3}. The carrier concentration was also deduced from a determination of the period $\Delta(1/H)$ of the SdH oscillations which yielded a Fermi energy, 36.2 meV, with an accuracy of 3%. From this value, n was calculated with Eq. (5) and was found to be in satisfactory agreement with the Hall-effect data. Since the Hall-coefficient factor r is equal to 1 for strongly degenerate semiconductors regardless of scattering mechanisms, the Hall data yielded the conductivity mobility. The reduced Fermi energy η at 4.2 K was 100 ± 3 for a set of six different samples.

B. Oscillatory Magnetoresistance

Figure 5 shows the Ohmic oscillatory longitudinal magnetoresistance up to 50 kG. There has been some discussion in the literature about the occurrence of spin splitting[35] in the longitudinal configuration; it was also suspected that contacts and geometrical effects may play an important role. Our sample geometry seems to exclude contact effects and Fig. 5 shows that spin splitting does occur in our samples in the longitudinal configuration. From this Ohmic measurement the Dingle temperature was determined by plotting $MH^{-1/2}\sinh\chi/\chi$ versus $1/H$. From the slope of this line a value of $T_D = 12.8\pm 0.5$ K is obtained. From a measurement of the oscillations in the transverse configuration the same value $T_D = 12.8\pm 1.0$ K was found (Fig. 6). Ohmic measurements were performed by applying electric fields having values less than 5 mV/cm to the samples. Application of higher electric fields caused damping of the oscillations in the longitudinal as well as the transverse configuration.

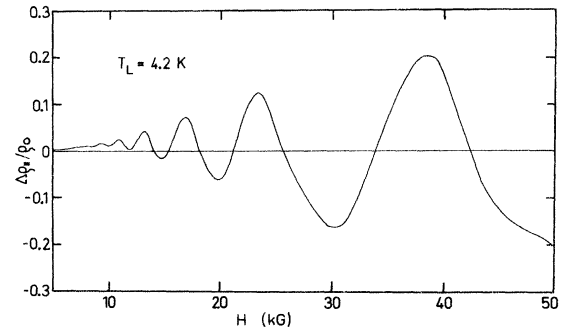

FIG. 5. Ohmic longitudinal magnetoresistance at 4.2 K.

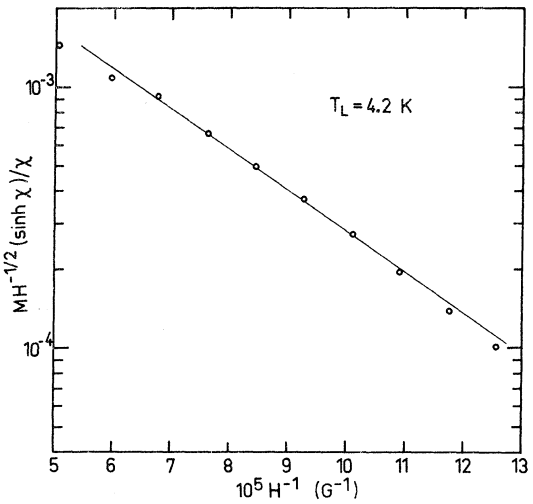

FIG. 6. Plot for a determination of the Dingle temperature.

The method for determining the dependence of the electron temperature on the electric field was presented in Refs. 24 and 25. With this method, electron temperatures were deduced from the longitudinal-configuration data. The influence of the electric field on the amplitude of the magnetoresistance oscillations was investigated up to electric fields of 2 V/cm. For this field strength the mobility variation for the $H = 0$ case is below 1% and therefore the assumption of a constant Dingle temperature is justified. We have also made a check of this assumption by deducing the Dingle temperature from the SdH amplitudes at higher electric fields after the determination of the electron temperature. Within the experimental error (1 K in the longitudinal configuration), T_D deduced at higher fields was the same as that for the Ohmic case.

The dependence of the amplitudes of the SdH oscillations on the electric field at different magnetic fields is shown in Figs. 7 and 8. From this variation, the dependence of the electron temperature on the electric field is deduced using Eq. (39), and shown in Fig. 9. There is a distinct kink in the rise of the electron temperature with electric field at about 400 mV/cm corresponding to $T_e \simeq 18$ K. The dependence of the electron temperature on the magnetic field for various electric fields is shown in Fig. 10. There is some indication for an oscillatory behavior of $T_e(H)$. Since these variations are small (< 5%) we have ignored

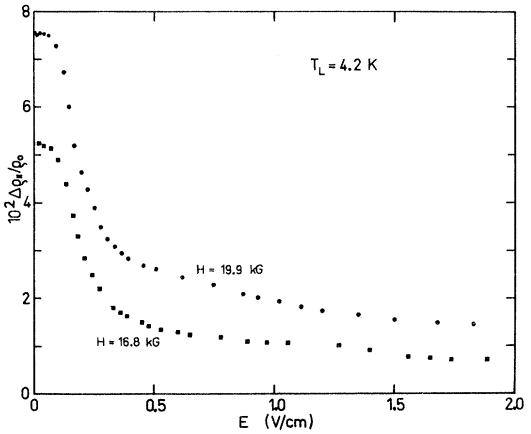

FIG. 7. Decrease of the amplitudes of the longitudinal SdH effect with electric field for $H = 19.9$ kG (solid circles) and $H = 16.8$ kG (solid squares).

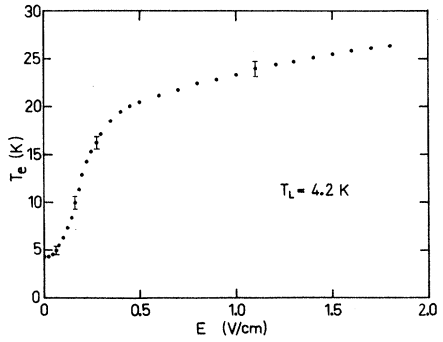

FIG. 9. Dependence of the electron temperature on the electric field at a lattice temperature of 4.2 K.

it and have related an average value of the electron temperature to each electric field regardless of the magnetic field. The electron temperatures in Fig. 9 were deduced by this procedure.

Measurements of $\Delta\rho/\rho_0(E, H)$ were also performed in the transverse configuration. Because of the appreciable nonoscillatory magnetoresistance in $E \perp H$, the electric field was not constant at different magnetic fields. An interpretation of the damping of the SdH amplitudes in terms of a unique electron temperature was not possible. From the increase of the electric field with increasing magnetic field (because of constant-current conditions) one would expect a relative decrease of the amplitudes because of an enhanced carrier heating. The opposite effect, namely, a relative increase of the amplitudes with increasing magnetic field, was observed, which is an indication of a cooling effect of the magnetic field in this configuration.

V. DISCUSSION

A. Applicability of Usual Transport-Theory Formalism

Ziman[14] has pointed out the extreme difficulties in accepting the Boltzmann equation unless Eqs. (2) and (3) are satisfied, since this treatment of transport is only applicable if the energy of an electron is perfectly defined. Using an effective mass of $m = 0.019 m_0$ at the Fermi level, we obtain from the mobility of our samples a value of $\tau = 9.35 \times 10^{-13}$ sec. Therefore we find $\hbar/\tau = 1.13 \times 10^{-15} \ll 5.8 \times 10^{-14}$ erg, which is the Fermi energy of our samples. With a Fermi velocity of $v_F = 8.2 \times 10^7$ cm/sec, we find the mean free path l_e to be 7.65×10^{-5} cm. Thus the product of l_e and the wave vector at the Fermi surface, $k_F = 1.23 \times 10^6$ cm^{-1}, has the value $k_F l_e = 94.3 \gg 1$. Conditions (2) and

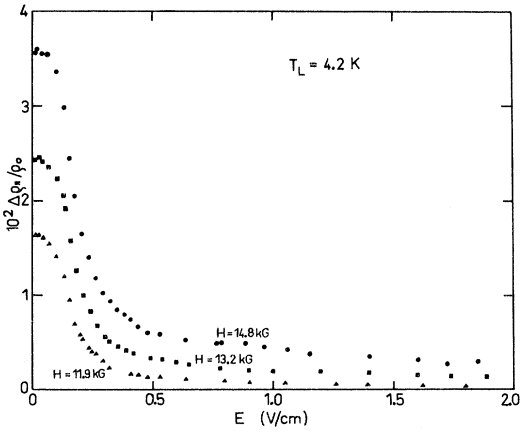

FIG. 8. Decrease of the amplitudes of the longitudinal SdH effect with electric field for $H = 14.8$ kG (solid circles), $H = 13.2$ kG (solid squares), and $H = 11.9$ kG (solid triangles).

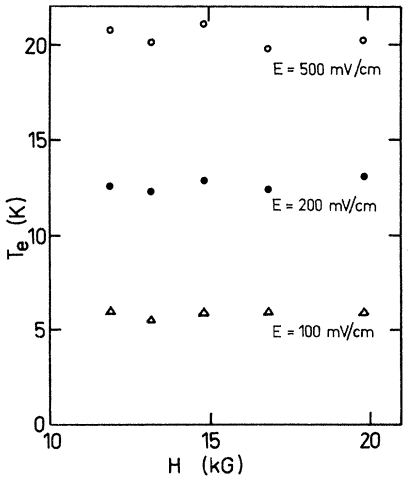

FIG. 10. Variation of electron temperature with magnetic field for $E = 100$ mV/cm (triangles), $E = 200$ mV/cm (solid circles), and $E = 500$ mV/cm (open circles).

(3) for the applicability of the usual formalism of transport theory are well satisfied for our samples.

Although Szymanska and Maneval[10] have noted the above difficulty, they have analyzed their data with the usual transport theory of Kogan.[12] For their sample parameters the conditions are $\hbar/\tau\epsilon_F = 0.4$ and $k_F l_e = 0.522$, posing serious questions for the applicability of the theory. The corresponding figures for the even lower mobility samples of Martin and Mead[11] are $\hbar/\tau\epsilon_F = 0.76$ and $k_F l_e = 0.28$. Similar criticism holds for the work by Kinch,[4,5] Lifshits *et al.*,[3] Whalen and Westgate,[36] and Crandall.[37] In a recent paper, Whalen and Westgate[36] have pointed out the impossibility of explaining measurements of the energy relaxation time τ_ϵ in InSb of a set of samples with different concentrations by a single set of coupling constants for acoustic scattering indicating the breakdown of the theoretical approach under conditions where Eqs. (1) or (2) and (3) are barely or not at all satisfied.

B. Ohmic Mobility

The mobility of the best samples was 74.500 cm^2/V sec. By chosing a proper value for $N_I = N_D + N_A$ to fit the theoretical value to the experimental data we have estimated the compensation ratio of our samples to have the remarkable low value of $N_A/N_D = 0.13$. The small dependence of the mobility on temperature which is characteristic for a highly degenerate material excluded the possibility of a determination of the field dependence of the electron temperature by comparing the dependence of the mobility on the lattice temperature and on the electric field.[8,25]

C. Energy-Loss Rate to Acoustic Phonons: Piezoelectric Coupling

In Table II we have compiled some experimental values of the piezoelectric-coupling coefficient e_{14} in InSb.[29,38–41] Table II does not aim at completeness, but demonstrates that this parameter is fairly well known from different appropriate experiments. Therefore, it seems to us not meaningful to use e_{14} as an adjustable parameter for a transport effect such as the energy-loss rate. We have calculated the average energy-loss rate per electron as a function of the electron temperature T_e according to the theory described in Sec. II. For the coupling constant we have inserted the value of 0.079 C/m^2.[29] The result of the numerical integration is shown in Fig. 11. For a calculation of the reduction of the energy-loss rate we have put $(|I_{1/2,1/2}|^2 + |I_{1/2,-1/2}|^2) = 1$. The p-function admixture weakens the electron-phonon interaction and decreases the energy-loss rate by approximately 26%. The influence of screening turned out to reduce the energy-loss rate by 20%. Figure 11 shows that the piezoelectric scattering below 12 K accounts for approximately only 20% of the experimentally observed energy-loss rate per electron which is the product $e\mu E^2$, E being the applied electric field.

TABLE II. Piezoelectric modulus of InSb.

e_{14} (C/m^2)	Experimental method	Ref.
0.060 ± 0.005	Microwave ultrasonic experiment	38
0.071 ± 0.007	Hybrid Hall-effect ultrasonic-wave technique	39
0.08	400–800-MHz ultrasonic study	40
0.079 ± 0.008	200-kHz resonant plate technique	29
0.076 ± 0.010	Ultrasonic-attenuation measurement	41

D. Energy-Loss Rate to Acoustic Phonons: Deformation-Potential Coupling

Contrary to the situation for the piezoelectric-coupling constant where different experiments have yielded values which are in satisfactory agreement, the value for the deformation-potential constant of the conduction band of InSb is still open to question. A fit of the temperature dependence of the mobility has been successful with values ranging from 7.2[42–44] up to 30 eV.[9,45] A fit of the energy-loss rate and the energy relaxation time at low temperatures was tried with values ranging from[36] 5 up to 30 eV.[5] From an analysis of infrared-absorption measurements, Haga and Kimura[46] found a value of 30 eV. Puri[47] found a value of 8.25 eV for the interpretation of his phonon-drag thermoelectric-power measurements. Tanaka *et al.*[48] have given a value of 16 eV from an investigation of the transverse acousto-conductive effect at low temperatures. Measurements of the shift of the plasma minimum with uniaxial stress in InSb by Zukotynski *et al.*[49] yielded a value of 25 eV. The ultrasonic study at 9 GHz by Nill and McWhorter produced 4.5 ± 0.5 eV,[38] whereas Smith *et al.*[41] have found a value of 5.8 eV for the sum of the deformation potentials of the conduction and valence bands. One of the most direct approaches to the deformation-potential constant is the measurement of the pressure dependence of the energy gap $(\partial\epsilon_g/\partial P)_T$ and of the compressibility K. With $|E_c + E_v| = (\partial\epsilon_g/\partial P)_T K^{-1}$, Ehrenreich[19] has given a value of $|E_c + E_v| = 7.2$ eV using Long's[50] data of $(\partial\epsilon_g/\partial P)_T$. It is beyond the scope of this paper to give a complete discussion of the various determinations of E_c. We want to point out, however, that in

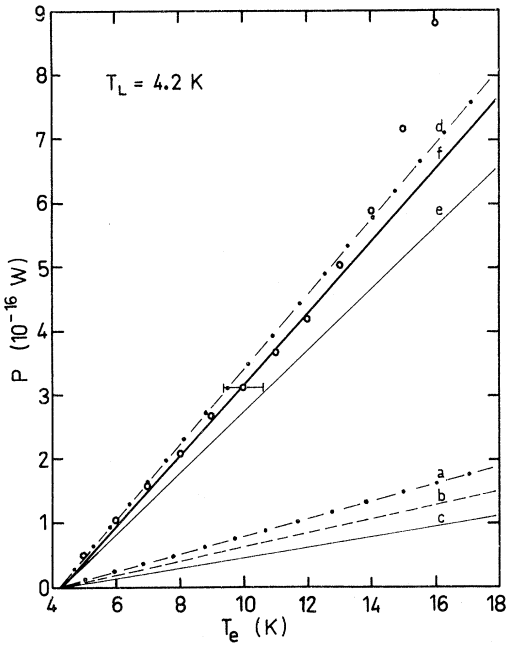

FIG. 11. Dependence of energy-loss rate P on the electron temperature. Curve (a): piezoelectric scattering, no screening, no p-function admixture; curve (b): with screening; curve (c): with screening and with p-function admixture; curve (d): deformation-potential scattering, no p-function admixture; curve (e): with p-function admixture; full curve (f): combination of both contributions (c) and (e); circles: experimental data taken from Fig. 9.

some cases the violation of the conditions for the applicability of the usual transport-theory formalism was either only mentioned or completely neglected. In particular this criticism applies to the work on non-Ohmic transport at low temperatures and to the investigation of the transverse acoustoconductive effect.[48]

Because of the above-described uncertainty of E_c we have used it as an adjustable parameter to fit the sum of the energy-loss rates for both types of acoustic scattering to the experimental data in Fig. 11. A best fit represented by the solid line in Fig. 11 was obtained with a value of $|E_c| = 6.9 \pm 0.4$ eV. According to the treatment by Zawadzki and Szymanska[21] we have neglected screening for this type of interaction but have considered a p-function admixture which decreases the energy-loss rate by approximately 19%. The contribution of the transverse modes was found to be nearly three orders of magnitude smaller than that of the longitudinal modes in the temperature range investigated. We also have studied the influence of screening by inserting a factor of $[\lambda^2 q^2/(1+\lambda^2 q^2)]^2$ into the integral of Eq. (28). The resulting reduction of the average energy-loss rate requires an increase of the deformation-potential constant to $|E_c| = 7.5 \pm 0.4$ eV to fit again the experimental data in Fig. 11 by combining both acoustic-phonon scattering mechanisms below 12 K.

The relative importance of piezoelectric scattering compared with deformation-potential scattering as shown in Fig. 11 is not a general result. It depends on the carrier concentration as indicated in Ref. 24. We have shown there that in the limit of strong degeneracy, the piezoelectric energy-loss rate per carrier P_{pi} is proportional to $n^{-1/3}$, whereas for deformation-potential scattering the energy-loss rate per carrier P_{def} is proportional to $n^{1/3}$. A crude estimate shows that both energy-loss rates are approximately equal for a carrier concentration of $n = 1\times 10^{16}$ cm^{-3}, whereas for $n = 1\times 10^{15}$ cm^{-3}, $P_{pi}/P_{def} \simeq 4$.

E. Energy-Loss Rate to Polar Optical Modes

Using a polar-optical-phonon Debye temperature of 278 K, we have calculated the average energy-loss rate for scattering by polar optical phonons as a function of T_e. Owing to the high ratio of the Debye temperature to the lattice temperature of 4.2 K, the absorption of polar optical phonons is negligibly small. The result of the calculations and the influence of p-function admixture and static screening on the energy-loss rate are shown in Fig. 12. The static-screening

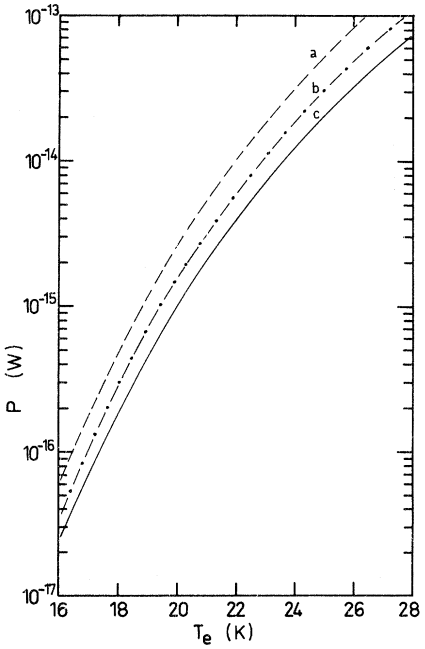

FIG. 12. Dependence of the energy-loss rate P for polar-optical-phonon scattering. Dashed curve (a): without screening and p-function admixture; dash-dotted curve (b): with screening; full curve (c): with screening and with p-function admixture.

treatment was first proposed by Ehrenreich[20] and adopted by Zawadzki and Szymanska.[21] Doniach[51] has proposed a dynamic treatment of screening which would have the opposite effect on mobility and energy-loss rate, namely, a decrease of the screened mobility and an increase of the energy-loss rate. We want to point out, however, that applying this treatment to our case would produce calculated energy-loss rates which are in excess of the experimentally observed values, thus destroying the agreement between experiment and theory at the highest electron temperatures achieved in this experiment.

In Fig. 13 the calculated temperature dependence of the energy-loss rate between 4.2 and 26 K is compared with the experimental values. The sum of the energy loss rates for deformation-potential and piezoelectric scattering is indicated together with the polar-optical-phonon energy-loss rate. At low and high temperatures the experimental points coincide with the calculation.

F. Discrepancies between Experiment and Theory

It is evident from Fig. 13 that in the temperature range between 14 and 22 K the experimental data of the energy-loss rate are higher than the sum of the contributions from deformation-potential, piezoelectric, and polar-optical-phonon scattering. That there exists a temperature range in which the experimentally determined energy-loss rate is higher than the acoustic energy-loss rate at temperatures where polar-optical-phonon scattering is not yet responsible for the energy dissipation is already known to occur in low-doped n-InSb.[6] Stradling and Wood[52] have pointed out that a process in which two transverse acoustic phonons of opposite wave vector having energies corresponding to the zone edge of the Brillouin zone would give good agreement with the experimentally observed magnetophonon effect at low temperatures. These authors have also tried to explain experiments like that of Sandercock[6] with this two-phonon-mechanism using a Debye temperature of 110 K for this process in InSb.

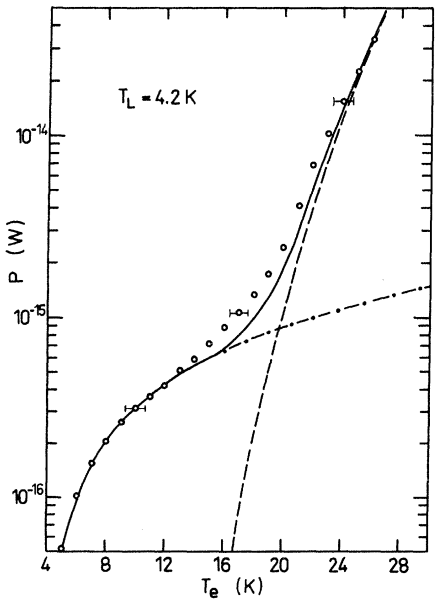

FIG. 13. Dependence of energy-loss rate P on electron temperature; dash-dotted curve: energy-loss rate due to the sum of both types of acoustic scattering; dashed curve: energy-loss rate owing to polar-optical-phonon scattering; solid curve: sum of acoustic and polar optical energy-loss rates; circles: experimental data taken from Fig. 9.

In Fig. 14 we have plotted the temperature dependence of the energy-loss process which one would need to add to the three above-mentioned mechanisms in order to explain the experimentally observed behavior. Unfortunately there exists no calculation of the matrix element for this two-phonon scattering process which considers the high density of phonon states in the vicinity of the Brillouin-zone edge. For n-type Ge, Alldredge and Blatt[53] have shown that the energy loss by two-phonon emission could become comparable to that involving the emission of single acoustic phonons.

Finally, we want to point out that the determination of the electron temperatures from the decrease of the SdH amplitudes requires a quantizing magnetic field. The calculation of the energy-loss rate described in this paper should therefore also take into account the influence of the magnetic field. A refinement of the theory for the energy-loss rate in a quantizing magnetic field for a degenerate electron gas under conditions where several Landau levels are occupied is very complicated. Our experiments (Fig. 10) show that the electron temperature and therefore the energy-loss rate do not depend significantly (< 5%) on the longitudinal magnetic field under these conditions. Thus we have neglected this small influence of the magnetic field on the temperature in our considerations.

VI. CONCLUSION

Integral expressions have been obtained for the energy-loss rates of the conduction electrons to the crystal lattice which take into account the nonparabolicity of the conduction band in InSb-type semiconductors, both in the density of states and in the electron wave functions. We have considered scattering by polar optical phonons and by acoustic phonons with deformation-potential and piezoelectric coupling. Static screening by the free electrons is included in the long-range interactions.

Numerical calculations of the various energy-

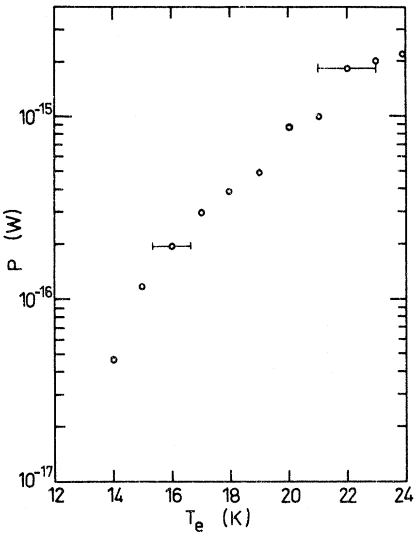

FIG. 14. Temperature dependence of additional energy-loss rate required to fit the experimental data to theory.

loss rates as a function of electron temperature were performed using the constants of the conduction band of InSb. The influence of screening and of the admixture of p-like components into the total wave function of the electron was investigated separately. The applicability of the usual formalism of transport theory for the interpretation of our experiments in InSb at 4.2 K was examined. We have shown that in sufficiently degenerate samples the well-known conditions are satisfied. With this knowledge, the calculated energy-loss rates are compared with the experimentally obtained dependence of the energy-loss rate on electron temperature which is deduced from an SdH experiment in pulsed electric fields. The decrease of the SdH amplitudes is used for the determination of the electron temperature. Below 12 K a combination of deformation-potential and piezoelectric scattering quantitatively fits the experimental data. The deformation-potential constant was used as a fitting parameter and a value of $|E_c| = 6.9 \pm 0.4$ eV was found in good agreement with a number of other independent investigations. Above 24 K, polar-optical-phonon scattering is shown to account for the energy-loss rate. In the intermediate range of temperatures between 14 and 24 K the discussed energy-loss mechanisms involving single-phonon interaction do not describe quantitatively the energy relaxation process. A possible explanation for the excess energy-loss rates in this temperature region might be a two-phonon process involving two transverse acoustic phonons at the zone edge of the Brillouin zone. The lack of knowledge of the interaction matrix element prevents a direct test for this assumption.

ACKNOWLEDGMENTS

The authors thank Professor K. Seeger for his continual interest and support of this work, Dr. P. Kocevar and Dr. K. Hess for valuable discussions, and Dr. M. V. Valenta for a critical reading of the manuscript. They also thank Dr. V. Dienys from the Institute of Semiconductor Physics of the Lithuanian Academy of Sciences, Vilnius, USSR, for fruitful cooperation in analyzing the experiments, and Dr. L. M. Bliek, PTB Braunschweig, for supplying the crystal. Numerical calculations were done at the Institut für Numerische Mathematik, T. H. Vienna.

*Work supported by the "Fonds zur Förderung der wissenschaftlichen Forschung" Austria, and the Ludwig Boltzmann Gesellschaft, Austria.

[1]For a review, see E. M. Conwell, in *Solid State Physics*, edited by F. Seitz, D. Turnbull, and H. Ehrenreich (Academic, New York, 1967), Suppl. 9.

[2]R. J. Sladek, Phys. Rev. 120, 1589 (1960).

[3]T. M. Lifshits, A. Ya. Oleinikov, and A. Ya. Shulman, Phys. Status Solidi 14, 511 (1966).

[4]M. A. Kinch, Brit. J. Appl. Phys. 17, 1257 (1966).

[5]M. A. Kinch, Proc. Phys. Soc. (London) 90, 819 (1967).

[6]J. R. Sandercock, Proc. Phys. Soc. (London) 86, 1221 (1965).

[7]J. J. Whalen and C. R. Westgate, Appl. Phys. Letters 15, 292 (1969).

[8]J. P. Maneval, A. Zylbersztejn, and H. F. Budd, Phys. Rev. Letters 23, 848 (1969).

[9]I. M. Tsidilkovskii and K. M. Demchuk, Phys. Status Solidi 44(b), 293 (1971).

[10]W. Szymanska and J. P. Maneval, Solid State Commun. 8, 879 (1970).

[11]J. P. Martin and J. B. Mead, Appl. Phys. Letters 17, 320 (1970).

[12]Sh. M. Kogan, Fiz. Tverd. Tela 4, 2474 (1962) [Sov. Phys. Solid State 4, 1813 (1963)].

[13]R. A. Stradling, L. Eaves, R. A. Hoult, A. L. Mears, and R. A. Wood, in *Proceedings of the International Conference on the Physics of Semiconductors, Cambridge*, 1970, edited by S. P. Keller, J. C. Hensel, and F. Stern, (US AEC, Oak Ridge, Tenn. 1970), p. 369.

[14]J. M. Ziman, *Electrons and Phonons* (Clarendon, Oxford, England, 1963).

[15]R. Peierls, Helv. Phys. Acta Suppl. 7, 24 (1934).

[16]R. Peierls, *Quantum Theory of Solids* (Oxford U.P., Oxford, England, 1955),

[17]J. B. Gunn, Phys. Rev. 138, A1721 (1965).

[18]E. O. Kane, Phys. Chem. Solids 1, 249 (1957).

[19]H. Ehrenreich, Phys. Chem. Solids 2, 131 (1957).

[20]H. Ehrenreich, Phys. Chem. Solids 9, 129 (1959).

[21]W. Zawadzki and W. Szymanska, Phys. Status Solidi 45(b), 415 (1971).

[22]T. Y. Stokoe and J. F. Cornwell, Phys. Status Solidi 49(b), 209 (1972).

[23]R. A. Isaacson and F. Bridges, Solid State Commun. 4, 635 (1966).

[24]H. Kahlert and G. Bauer, Phys. Status Solidi 46(b), 535 (1971).
[25]G. Bauer and H. Kahlert, Phys. Rev. B 5, 566 (1972).
[26]J. Kolodziejczak, Acta Phys. Polon. 20, 289 (1961).
[27]W. Zawadzki and W. Szymanska, J. Phys. Chem. Solids 32, 1151 (1971).
[28]E. J. Johnson and D. H. Dickey, Phys. Rev. B 3, 2676 (1970).
[29]A. Arnaud and G. Quentin, Phys. Letters 32A, 16 (1970).
[30]M. Hass, in *Semiconductors and Semimetals*, edited by R. K. Willardson and A. C. Beer (Academic, New York, 1967), Vol. 3, p. 14.
[31]S. Zwerdling, W. H. Kleiner, and J. P. Theriault, J. Appl. Phys. Suppl. 32, 2118 (1961).
[32]R. R. L. Zucca and Y. R. Shen, Phys. Rev. B 3, 2668 (1970).
[33]D. Matz, Phys. Rev. 168, 843 (1968).
[34]L. M. Roth and P. N. Argyres, in *Semiconductors and Semimetals*, edited by R. K. Willardson and A. C. Beer (Academic, New York, 1966), Vol. 1, p. 159.
[35]L. M. Bliek, G. Landwehr, and M. v. Ortenberg, in *Proceedings of the International Conference on the Physics of Semiconductors, Moscow* 1968, edited by S. M. Ryvkin (Nauka, Leningrad, 1969), p. 710.
[36]J. J. Whalen and C. R. Westgate, J. Appl. Phys. 43, 1965 (1972).
[37]R. S. Crandall, Solid State Commun. 7, 1575 (1969).
[38]K. W. Nill and A. L. McWhorter, J. Phys. Soc. Japan Suppl. 21, 755 (1966).
[39]G. Arlt and P. Quadflieg, Phys. Status Solidi 25, 323 (1968).
[40]I. L. Drichko, Y. V. Ilisavskii, and Y. M. Galperin, Fiz. Tverd. Tela 11, 2463 (1969) [Sov. Phys. Solid State 11, 1989 (1970)].
[41]W. D. Smith, J. G. Miller, R. K. Sundfors, and D. I. Bolef, J. Appl. Phys. 42, 2579 (1971).
[42]D. L. Rode, Phys. Rev. B 2, 1012 (1970).
[43]D. Kranzer and E. Gornik, Solid State Commun. 9, 1541 (1971).
[44]V. V. Galavanov, D. N. Nasledov, and A. S. Filipchenko, Phys. Status Solidi 8, 671 (1965).
[45]F. Buchy, Phys. Status Solidi 10, K3 (1965).
[46]E. Haga and H. Kimura, J. Phys. Soc. Japan 18, 777 (1963).
[47]S. M. Puri, Phys. Rev. 139, A995 (1965).
[48]S. Tanaka, S. Asai, and M. Kogami, in Ref. 35, p. 779.
[49]S. Zukotynski, S. Graf, and N. Saleh, Phys. Status Solidi 42, K43 (1970).
[50]D. Long, Phys. Rev. 99, 388 (1955).
[51]S. Doniach, Proc. Phys. Soc. (London) 73, 849 (1959).
[52]R. A. Stradling and R. A. Wood, J. Phys. C 3, 2425 (1970).
[53]G. P. Alldredge and F. J. Blatt, Ann. Phys. (N. Y.) 45, 191 (1967).

PHYSICAL REVIEW B VOLUME 7, NUMBER 6 15 MARCH 1973

Brillouin-Scattering Study of Propagating Acoustoelectric Domains in Semiconducting CdS†

Masayoshi Yamada,* Chihiro Hamaguchi, Kazuhisa Matsumoto, and Junkichi Nakai
Department of Electronics, Faculty of Engineering, Osaka University, Suita, Osaka, Japan
(Received 2 March 1972; revised manuscript received 7 July 1972)

Brillouin scattering in an anisotropic medium is developed by taking account of the off-axis effect, and some aspects of amplified shear waves in propagating acoustoelectric domains in semiconducting CdS are presented. The small-signal theory for piezoelectrically active waves amplified from the thermal background of lattice vibrations is formalized by taking account of nonelectronic lattice loss. When the acoustic flux intensity was less than about 10^{-3} J/cm^3, the growth rate and frequency dependence of the on-axis components of acoustic flux were all found to be consistent with the small-signal theory. As for the off-axis components, the angular distribution of the acoustic flux, angular dependence of net gain coefficient, and narrowing of the cone of the acoustic flux also gave a reasonably good agreement with the theory. However, they have been strongly subjected to the influence of the nonelectronic-lattice-loss term. Using a dual-pulse method, it was found that the frequency dependence of the attenuation of acoustic flux was proportional to $f^{1.5}$ and its angular dependence proportional to the square of the off-axis angle. The angular dependence of the nonelectronic lattice loss was tentatively explained with the help of boundary scattering. In the subsequent stages of growth, when the acoustic waves became very intense, many interesting nonlinear effects were found in contrast to the small-signal theory. The acoustic spectrum was rapidly extended to both low and high frequencies, compared with that as expected under the small-signal condition. The subharmonic was strongly amplified and its growth rate became three times larger than that of initially amplified flux. There was a reasonably large growth rate even at high frequencies.

I. INTRODUCTION

It is well known that energy and momentum are transferred from the mobile charge carriers to the acoustic waves when the drift velocity exceeds the sound velocity by the application of a sufficiently high electric field.[1,2] The electrical instabilities caused by such interactions of electrons or holes with internally generated acoustic waves have been observed in many piezoelectric semiconductors[3]